ACS Macro Letters

pubs.acs.org/macroletters Letter

Preparation, Characterization, and Self-Assembly of P3HT-Based Janus Fibers via a Crystallization-Driven Self-Assembly Process

Boyang Shi, Chengcheng Zhou, Xinyu Wang, Ding Shen, and Guowei Wang*

Cite This: ACS Macro Lett. 2025, 14, 1367−1374 Read Online

ACCESS | Metrics & More | Article Recommendations | Supporting Information

ABSTRACT: Poly(3-hexylthiophene) (P3HT)-based complex topological copolymers have attracted a great deal of attention for their unique electrical and optical properties. In this contribution, the P3HT-based Janus fibers with controlled lengths were innovatively prepared by sequential crystallization-driven self-assembly (CDSA) of poly(*p*-*tert*-butylstyrene)-*b*-polyisoprene-*b*-poly(3-hexylthiophene) (P*t*BS-*b*-PI-*b*-P3HT) triblock copolymer, cross-linking of the interlayer PI region, and dissociation of fibers in good solvent. The comprehensive characterizations showed that the P*t*BS/P3HT Janus fibers have nearly half the width of P*t*BS-*b*-PI-*b*-P3HT fibers and fiber lengths close to or slightly shorter than those of P*t*BS-*b*-PI-*b*-P3HT fibers, indicating that the Janus fibers with adjustable lengths could be prepared in a large window range. Furthermore, the P*t*BS/P3HT Janus fibers could re-self-assemble into average 2- or 4-aggregates in selective solvent. The work provided a general strategy to produce P3HT-based or analogous π-conjugated polymer-based Janus fibers, which is hoped to facilitate the applications of π-conjugated polymers in advanced materials.

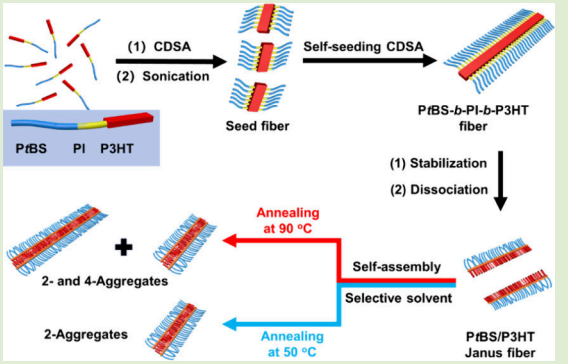

Poly(3-hexylthiophene) (P3HT) has been widely studied for its excellent electrical and optical properties, as well as its solubility, environmental stability, and synthetic availability.[1−6] The P3HT-based linear,[6−11] cyclic,[12,13] starlike,[14,15] hyperbranched[16] and bottlebrush[17−23] rod−coil (co)polymers have also been purposefully developed to improve the properties of P3HT. Among these P3HT-based (co)polymers, the bottlebrush (co)polymer was especially favored due to its low chain entanglement and high elasticity.[19,24] For example, Wong et al. synthesized P3HT-based bottlebrush (co)polymer via ring opening metathesis polymerization (ROMP) of P3HT-based norbornene macromonomer.[17] Thelakkat et al. synthesized P3HT-based bottlebrush of polystyrene-*g*-poly(3-hexylthiophene) (PS-*g*-P3HT) via grafting-onto approach using a "click" reaction.[23] Both works showed that the bottlebrush (co)polymers with P3HT side chains could impart better charge transport properties. Among the bottlebrush (co)polymer, the Janus bottlebrush is a class of macromolecular brush with two different side chains on the same repeating unit of backbone.[25] The special asymmetrical architecture endows these Janus (co)polymer with an ideal capacity of phase separation, as well as unique properties.[25−29]

Generally, the bottlebrush (co)polymers can be prepared by grafting-from, grafting-onto, and grafting-through methodologies.[20,25,30] However, the low efficiency of grafting and the complicated synthetic procedure of macromonomers limit their application in preparing bottlebrush (co)polymers.[31] Especially, for Janus bottlebrush (co)polymer, the synthesis of two-component macromonomers is necessary for grafting-through strategy, while multiple active sites and sophisticated steps are necessary for grafting-from and/or grafting-onto strategies.[25] Alternatively, as analogues to Janus bottlebrush (co)polymers, the Janus fibers can be fabricated via a self-assembly process.[32−34] Especially, the crystallization-driven self-assembly (CDSA) technique has greatly facilitated the preparation of Janus fibers due to its function on obtaining the well-defined one-dimensional (1D) or two-dimensional (2D) nano-objects.[27,34] For example, Li et al. prepared pH-responsive Janus (co)polymer nanoplates via CDSA of poly(ε-caprolactone)-*b*-poly(acrylic acid) (PCL-*b*-PAA), followed by a cross-linking PAA block and a dissociation process.[34] Schmalz et al. prepared Janus fibers based on direct CDSA of polystyrene-*b*-polyethylene-*b*-poly(ethylene oxide) (PS-*b*-PE-*b*-PEO) triblock copolymer.[27] However, the P3HT-based Janus bottlebrush (co)polymers or analogous Janus fibers were rarely reported in the literature. The realization of such structures may maximally fulfill the excellent function of P3HT block. Coincidentally, π-conjugated P3HT-based block copolymers prefer to form fibers with a crystalline P3HT core

Received: August 9, 2025
Revised: September 2, 2025
Accepted: September 3, 2025
Published: September 9, 2025

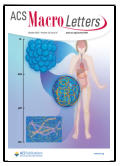

https://doi.org/10.1021/acsmacrolett.5c00525
ACS Macro Lett. 2025, 14, 1367−1374

Scheme 1. Synthetic Procedure for P*t*BS/P3HT Janus Fibers and the Precursors

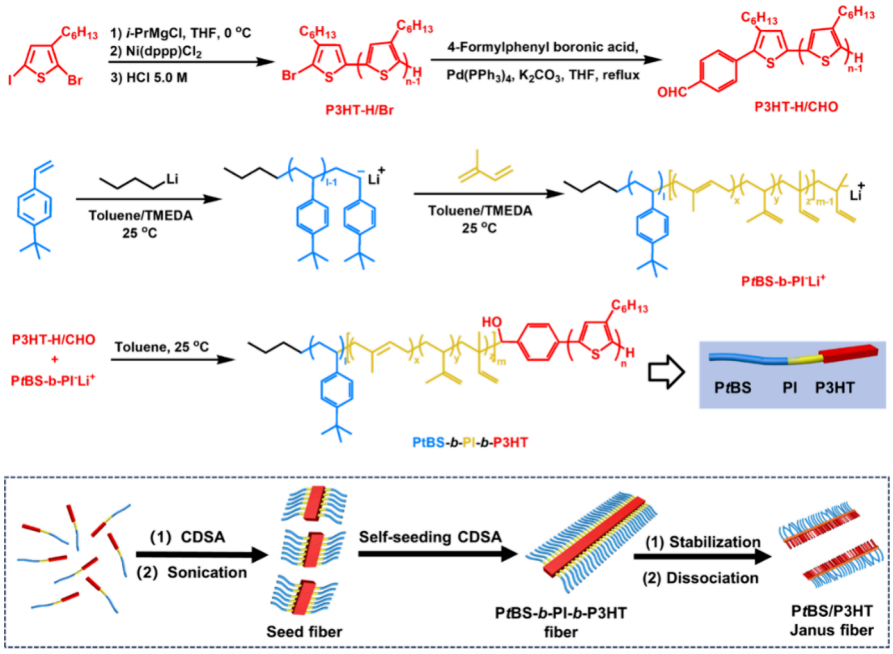

via the CDSA process, which provides possibilities for preparing the Janus fibers.[35−44]

Herein, we developed a versatile strategy for preparing P3HT-based Janus fibers. Generally, the poly(*p*-*tert*-butylstyrene)-*b*-polyisoprene-*b*-poly(3-hexylthiophene) (P*t*BS-*b*-PI-*b*-P3HT) triblock copolymer was synthesized and self-assembled as nanofibers with P3HT as the core region, PI as the interlayer, and P*t*BS as the outer stabilizer via a typical CDSA process. After a sonication process and a subsequent self-seeding CDSA process, a series of nanofibers with controllable lengths were generated. Following a cross-linking reaction of the PI interlayer via hydrosilylation reaction and dissociation of the assemblies, the P*t*BS/P3HT Janus fibers were finally obtained (Scheme 1).

As an example, the P*t*BS$_{89}$-*b*-PI$_{68}$-*b*-P3HT$_{35}$ triblock copolymer was first prepared according to the literature[45,46] and was characterized by size exclusion chromatography (SEC), proton nuclear magnetic resonance (^{1}H NMR), and matrix-assisted laser desorption/ionization time-of-flight mass spectrometry (MALDI-TOF MS) measurements (Figures S1−S5), respectively. Subsequently, the P*t*BS$_{89}$-*b*-PI$_{68}$-*b*-P3HT$_{35}$ nano-objects were generated by a typical CDSA process in *n*-heptane/toluene (Hep/Tol, 9/1, v/v). The original P*t*BS$_{89}$-*b*-PI$_{68}$-*b*-P3HT$_{35}$ fibers with a width of 21 nm and a number-average length (L_n) of around 500 nm were formed (Figure S6). Furthermore, the original P*t*BS$_{89}$-*b*-PI$_{68}$-*b*-P3HT$_{35}$ fibers were fragmented with sonication, and seed fibers with a width of 21 nm and a L_n of 100 nm were obtained (Figure 1a). To prepare the P*t*BS$_{89}$-*b*-PI$_{68}$-*b*-P3HT$_{35}$ fibers with controlled lengths, the self-seeding of the seed fibers was conducted by thermal annealing the aliquots at different temperatures (from 50 to 90 °C). The TEM images showed that (Figures 1b−g and S7) the L_ns of the corresponding regenerated fibers regularly ranged from 134 to 563 nm with an increase in the annealing temperatures, and the distributions of the length (L_w/L_n) for those fibers were all under 1.20. These results followed the typical feature of self-seeding CDSA as the fraction of surviving seed fibers decreased with the increase of annealing temperatures, and thus, more unimers could grow onto the seed fibers.[40,47,48] Meanwhile, the DLS curves showed a tendency consistent with those from the TEM measurement (Figure 1h), further confirming the successful preparation of the P*t*BS$_{89}$-*b*-PI$_{68}$-*b*-P3HT$_{35}$ fibers with controlled L_ns, as illustrated in Figure 1i.

Based on the different solubilities of P*t*BS, PI and P3HT blocks in Hep/Tol (9/1, v/v) cosolvent and the defined topology of the P*t*BS$_{89}$-*b*-PI$_{68}$-*b*-P3HT$_{35}$ triblock copolymer, it could be deduced that the P3HT formed the core region, the PI served as the interlayer, and the P*t*BS acted as the stabilizer in the P*t*BS$_{89}$-*b*-PI$_{68}$-*b*-P3HT$_{35}$ fibers. Thus, the P*t*BS$_{89}$-*b*-PI$_{68}$-*b*-P3HT$_{35}$ fibers could be stabilized by cross-linking the double bonds in the PI interlayer. For this aim, the hydrosilylation reaction was selected to achieve the intramicellar cross-linking reaction in P*t*BS$_{89}$-*b*-PI$_{68}$-*b*-P3HT$_{35}$ fibers, employing 1,1,3,3-tetramethyl disiloxane as the cross-linker and Karstedt's catalyst as the promoter at 40 °C for 4 days. Correspondingly, the stabilized P*t*BS$_{89}$-*b*-PI$_{68}$-*b*-P3HT$_{35}$ fibers were dissociated in good solvent and the P*t*BS$_{89}$/P3HT$_{35}$ Janus fibers were obtained. As the ^{1}H NMR spectrum shows in Figure S8, in a good solvent, such as $CDCl_3$, the resonance signals between 4.5 and 6.0 ppm are attributed to the protons (−C***H***=C***H***$_2$, -C***H*** (CH_3)=C***H***-, -C***H*** (CH_3)=C***H***$_2$) on the double bonds of the PI block, which were obviously attenuated for the P*t*BS$_{89}$/P3HT$_{35}$ Janus fibers compared with that for the precursor of P*t*BS$_{89}$-*b*-PI$_{68}$-*b*-P3HT$_{35}$, and ca. 24% of the double bonds were consumed. As shown in Figure 2a−e, in a good solvent, such as toluene, all these P*t*BS$_{89}$/P3HT$_{35}$ Janus fibers maintained an independent fibrous morphology. Differently, the unstabilized P*t*BS$_{89}$-*b*-PI$_{68}$-*b*-P3HT$_{35}$ fibers showed weak aggregates in toluene, and no regular morphologies could be discriminated (Figure 2f). On the one hand, compared with the P*t*BS$_{89}$-*b*-PI$_{68}$-*b*-P3HT$_{35}$ fibers annealed from 50, 60, and 70 °C in Hep/Tol (9/1, v/v) cosolvent (Figure S7), the corresponding P*t*BS$_{89}$/P3HT$_{35}$ Janus fibers in toluene had similar but slightly increased L_ns from 134 to 161, 159 to 190, and 209 to 212 nm, respectively (Figures 2g and S9), which

https://doi.org/10.1021/acsmacrolett.5c00525
ACS Macro Lett. 2025, 14, 1367−1374

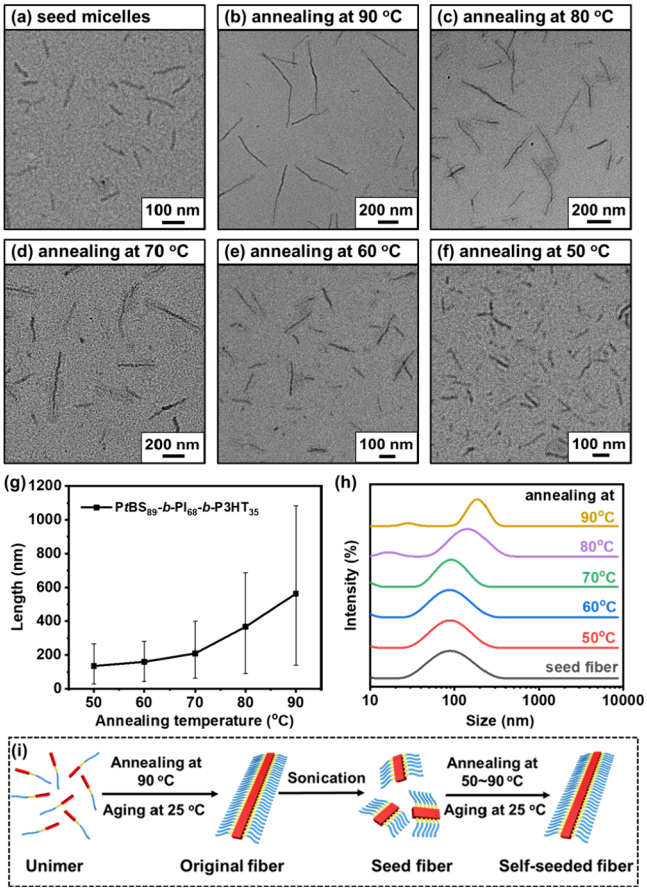

Figure 1. TEM images of nano-objects (diluted into 0.04 mg/mL dispersions in Hep/Tol (9/1, v/v) cosolvent) (a) formed by the CDSA of P*t*BS$_{89}$-*b*-PI$_{68}$-*b*-P3HT$_{35}$, annealed at 90 °C and fragmented with sonication at 25 °C, and those via self-seeding CDSA with annealing temperatures at (b) 90, (c) 80, (d) 70, (e) 60, and (f) 50 °C, respectively. (g) L_n of fibers vs annealing temperatures. (h) DLS results of the corresponding nano-objects. (i) Schematic illustration of the formation of P*t*BS$_{89}$-*b*-PI$_{68}$-*b*-P3HT$_{35}$ fibers via CDSA and self-seeding CDSA process.

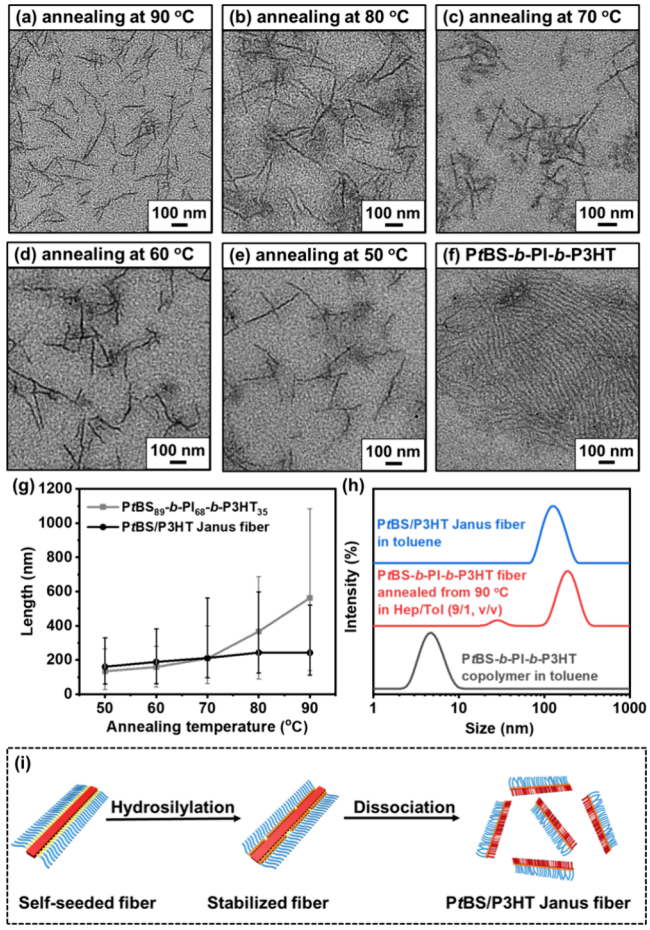

Figure 2. TEM images of the P*t*BS/P3HT Janus fibers (diluted into 0.04 mg/mL dispersions in toluene) by annealing the P*t*BS$_{89}$-*b*-PI$_{68}$-*b*-P3HT$_{35}$ fibers at (a) 90, (b) 80, (c) 70, (d) 60, and (e) 50 °C, respectively, and (f) the weak aggregates formed by the self-assembly of P*t*BS$_{89}$-*b*-PI$_{68}$-*b*-P3HT$_{35}$ in toluene. (g) L_n of P*t*BS/P3HT Janus fibers and P*t*BS$_{89}$-*b*-PI$_{68}$-*b*-P3HT$_{35}$ fibers vs annealing temperatures. (h) DLS results of the corresponding copolymers and fibers. (i) Schematic illustration of the formation of P*t*BS/P3HT Janus fibers via cross-linking and dissociation processes.

indicated that the P*t*BS$_{89}$-*b*-PI$_{68}$-*b*-P3HT$_{35}$ fibers with L_ns under 200 nm could be sufficiently stabilized. However, when the L_ns of P*t*BS$_{89}$-*b*-PI$_{68}$-*b*-P3HT$_{35}$ fibers were over 200 nm after annealing at 80 and 90 °C in Hep/Tol (9/1, v/v) cosolvent, the cross-linking reaction became discontinuous, causing the fractured P*t*BS$_{89}$/P3HT$_{35}$ Janus fibers in toluene with a relatively constant L_n of around 240 nm (Figures 2g and S9). Nevertheless, the L_w/L_ns for the stabilized fibers were maintained below 1.25 in all cases. On the other hand, the width of the P*t*BS$_{89}$/P3HT$_{35}$ Janus fibers was approximately 12 nm, nearly half that of the P*t*BS$_{89}$-*b*-PI$_{68}$-*b*-P3HT$_{35}$ fibers. According to refs 49 and 50, the P3HT chains with a molecular weight (MW) below 10 kDa did not have chain-fold, instead forming lamellar crystals via the stacking of fully extended chains in the CDSA system. This meant that the 1D fibers made by P3HT-based block copolymers were actually ribbon-like rather than cylindrical. Thus, for P*t*BS$_{89}$-*b*-PI$_{68}$-*b*-P3HT$_{35}$ fibers, the P*t*BS$_{89}$-*b*-PI$_{68}$ shell is distributed on both sides of the crystalline P3HT core as illustrated in Figures 1i and 2i. The PI block on both sides of the stabilized P*t*BS$_{89}$-*b*-PI$_{68}$-*b*-P3HT$_{35}$ fibers was cross-linked independently during the hydrosilylation reaction. When the cross-linked fibers were dissociated, the P*t*BS$_{89}$/P3HT$_{35}$ Janus fibers were thus formed with one side of P*t*BS and another side of P3HT (Figure 2i). Correspondingly, the P*t*BS$_{89}$/P3HT$_{35}$ Janus fibers were discriminated with nearly half the width of that for the P*t*BS$_{89}$-*b*-PI$_{68}$-*b*-P3HT$_{35}$ fibers. The sizes of P*t*BS$_{89}$-*b*-PI$_{68}$-*b*-P3HT$_{35}$ fibers and P*t*BS$_{89}$/P3HT$_{35}$ Janus fibers were also monitored by DLS measurement. As an example, after annealing at 90 °C, the DLS curve showed that the size of the P*t*BS$_{89}$/P3HT$_{35}$ Janus fibers in toluene was 120 nm, which was slightly smaller than that of the P*t*BS$_{89}$-*b*-PI$_{68}$-*b*-P3HT$_{35}$ fibers (200 nm) formed in Hep/Tol (9/1, v/v) cosolvent. Conversely, the size of the P*t*BS$_{89}$/P3HT$_{35}$ Janus fibers in toluene was obviously larger than that of the dissolved P*t*BS$_{89}$-*b*-PI$_{68}$-*b*-P3HT$_{35}$ triblock copolymer in toluene (5 nm, Figure 2h). These results confirmed the successful preparation of the stabilized P*t*BS$_{89}$/P3HT$_{35}$ Janus fibers.

Meanwhile, after annealing at 90 °C, the morphologies and sizes of P*t*BS$_{89}$-*b*-PI$_{68}$-*b*-P3HT$_{35}$ fibers and P*t*BS$_{89}$/P3HT$_{35}$ Janus fibers in solution were monitored by AFM and SEM measurements, respectively. The AFM measurement showed that the width of the P*t*BS$_{89}$-*b*-PI$_{68}$-*b*-P3HT$_{35}$ fibers was measured to be about 61 nm, while that of the P*t*BS$_{89}$/P3HT$_{35}$

https://doi.org/10.1021/acsmacrolett.5c00525
ACS Macro Lett. 2025, 14, 1367−1374

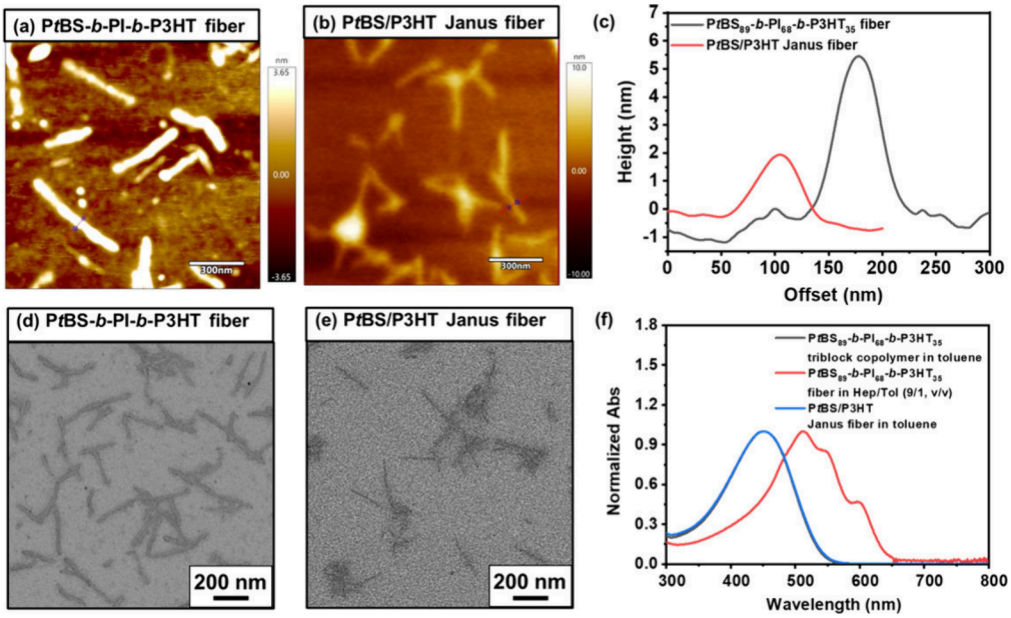

Figure 3. AFM images of (a) P*t*BS$_{89}$-*b*-PI$_{68}$-*b*-P3HT$_{35}$ fibers in Hep/Tol (9/1, v/v) cosolvent, (b) P*t*BS/P3HT Janus fibers in toluene, and the (c) high profile of the corresponding fibers. SEM images of (d) P*t*BS$_{89}$-*b*-PI$_{68}$-*b*-P3HT$_{35}$ fibers in Hep/Tol (9/1, v/v) cosolvent, and (e) P*t*BS/P3HT Janus fibers in toluene. (f) UV−vis spectra for the corresponding copolymers and fibers.

Janus fibers was about 42 nm. The P*t*BS$_{89}$-*b*-PI$_{68}$-*b*-P3HT$_{35}$ fibers had a height of 5−6 nm, while the P*t*BS$_{89}$/P3HT$_{35}$ Janus fibers had a height of 2 nm (Figure 3a−c). Similar results were also obtained by SEM measurement, which showed that the P*t*BS$_{89}$-*b*-PI$_{68}$-*b*-P3HT$_{35}$ fibers had an average width of 39 nm, while the P*t*BS$_{89}$/P3HT$_{35}$ Janus fibers had an average width of 22 nm (Figure 3d,e). The fiber widths measured by TEM, SEM, and AFM measurements were different, which could be attributed to the different sampling methods and test principles. Nevertheless, all of the results indicated that the width of P*t*BS$_{89}$/P3HT$_{35}$ Janus fibers was almost half that of P*t*BS$_{89}$-*b*-PI$_{68}$-*b*-P3HT$_{35}$ fibers, which was consistent with the theoretical assumption. The UV−vis analysis was also performed on P*t*BS$_{89}$/P3HT$_{35}$ Janus fibers. As shown in Figure 3f, the P*t*BS$_{89}$/P3HT$_{35}$ Janus fibers had the same maximum absorption wavelength (λ_{max}) at 450 nm as the P*t*BS$_{89}$-*b*-PI$_{68}$-*b*-P3HT$_{35}$ had in toluene, while P*t*BS$_{89}$-*b*-PI$_{68}$-*b*-P3HT$_{35}$ fibers had a red-shifted λ_{max} at 515 nm in Hep/Tol (9/1, v/v) cosolvent. Although restricted in a Janus structure, the P3HT in P*t*BS$_{89}$/P3HT$_{35}$ Janus fibers had similar solubility and chain mobility in toluene as the triblock copolymers had, rather than a crystallized state like those in Hep/Tol (9/1, v/v) cosolvent.

The thermal properties of the P*t*BS$_{89}$-*b*-PI$_{68}$-*b*-P3HT$_{35}$ triblock copolymer and the P*t*BS$_{89}$/P3HT$_{35}$ Janus fibers in the bulk state were studied and compared by differential scanning calorimetry (DSC) analysis. For P*t*BS$_{89}$-*b*-PI$_{68}$-*b*-P3HT$_{35}$, the glass transition temperature (T_g) of the P*t*BS and PI blocks could not be discerned due to the low MWs. Clearly, in the first cooling run (Figure 4a), the P*t*BS$_{89}$-*b*-PI$_{68}$-*b*-P3HT$_{35}$ showed a single crystallization temperature (T_c) at 165.2 °C, while P*t*BS$_{89}$/P3HT$_{35}$ Janus fibers had multiple crystalline peaks with relatively lower T_cs between 140.3 and 165.0 °C. The T_cs of P*t*BS$_{89}$/P3HT$_{35}$ Janus fibers were regularly increased with the increase of the annealing temperatures for P*t*BS$_{89}$-*b*-PI$_{68}$-*b*-P3HT$_{35}$ fibers. A similar tendency could also be observed in the second heating run

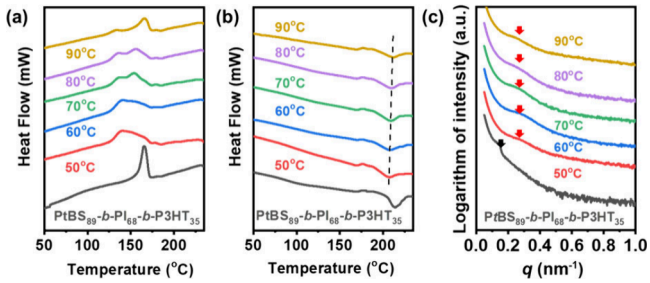

Figure 4. DSC traces for the P*t*BS$_{89}$-*b*-PI$_{68}$-*b*-P3HT$_{35}$ triblock copolymer and P*t*BS/P3HT Janus fibers formed from different annealing temperatures: (a) the first cooling run; (b) the second heating run. (c) SAXS profiles for the corresponding copolymers and fibers.

(Figure 4b). The melting temperature (T_m) of P3HT in P*t*BS$_{89}$-*b*-PI$_{68}$-*b*-P3HT$_{35}$ was detected at 214.0 °C, while T_ms of P*t*BS$_{89}$/P3HT$_{35}$ Janus fibers were lower and observed between 210.5 and 204.0 °C. The melting enthalpies were also decreased from 5.5 J/g for P*t*BS$_{89}$-*b*-PI$_{68}$-*b*-P3HT$_{35}$ to below 3.8 J/g for P*t*BS$_{89}$/P3HT$_{35}$ Janus fibers. The decreased T_c, T_m, and melting enthalpies indicated that the crystallinity of P3HT in P*t*BS$_{89}$/P3HT$_{35}$ Janus fibers was relatively decreased due to the weakened mobility of the P3HT side chain in the bulk state.[51] Regularly, the longer P*t*BS$_{89}$/P3HT$_{35}$ Janus fibers contributed to higher T_cs or T_ms. It could be presumed that the longer Janus fiber provided a relatively larger ordered space for the crystallization of the P3HT block.

The P*t*BS$_{89}$-*b*-PI$_{68}$-*b*-P3HT$_{35}$ triblock copolymer and P*t*BS$_{89}$/P3HT$_{35}$ Janus fibers in the bulk state were also characterized by wide-angle X-ray scattering (WAXS) and small-angle X-ray scattering (SAXS) analyses, respectively. As shown in Figure S10, the WAXS diffraction pattern showed the (100) reflection peak at 2θ = 5.4° and the (010) reflection peak at 2θ = 23.2° for P3HT$_{35}$ in P*t*BS$_{89}$-*b*-PI$_{68}$-*b*-P3HT$_{35}$. The broad peak from 12° to 20° belonged to the amorphous P*t*BS and PI blocks.[52] Compared with P*t*BS$_{89}$-*b*-PI$_{68}$-*b*-P3HT$_{35}$, the

https://doi.org/10.1021/acsmacrolett.5c00525
ACS Macro Lett. 2025, 14, 1367−1374

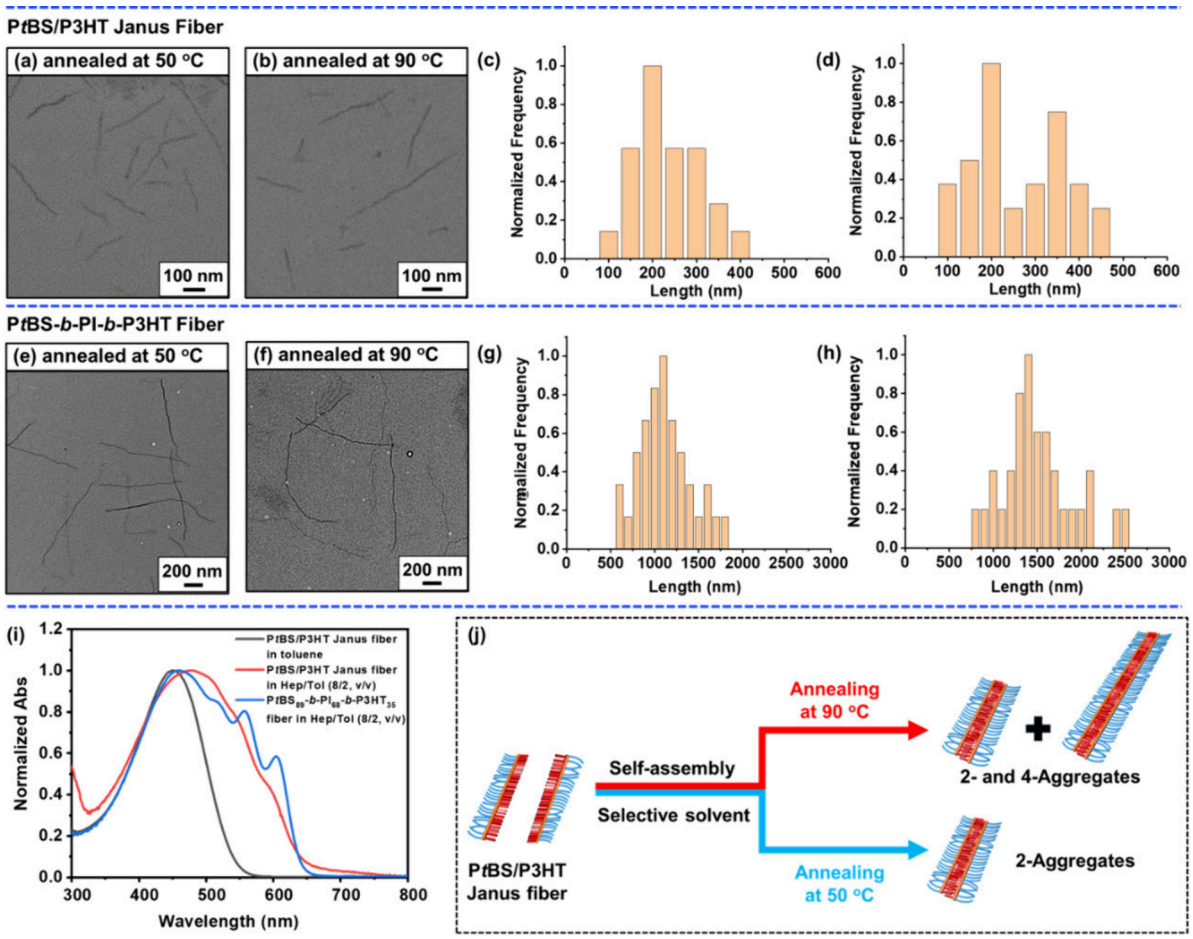

Figure 5. TEM images of nano-objects (diluted into 0.04 mg/mL dispersions) formed by the re-self-assembly of P*t*BS/P3HT Janus fibers and CDSA of P*t*BS$_{89}$-*b*-PI$_{68}$-*b*-P3HT$_{35}$ triblock copolymer in Hep/Tol (8/2, v/v) cosolvent after annealing at 50 (a, e) and 90 °C (d, f), respectively. The histograms of the contour length distribution of the corresponding fibers at 50 (c, g) and (d, h) 90 °C, respectively. (i) UV−vis spectra for the corresponding fibers. (j) Schematic illustration of the re-self-assembly of P*t*BS/P3HT Janus fibers.

P*t*BS$_{89}$/P3HT$_{35}$ Janus fibers revealed the attenuation of both reflection peaks at $2\theta = 5.4°$ and $2\theta = 23.2°$. The SAXS profiles showed a broad peak around $q = 0.15$ nm^{-1} for P*t*BS$_{89}$-*b*-PI$_{68}$-*b*-P3HT$_{35}$ and 0.27 nm^{-1} for P*t*BS$_{89}$/P3HT$_{35}$ Janus fibers (Figure 4c). The larger q indicated that the smaller disordered regions as P*t*BS$_{89}$/P3HT$_{35}$ Janus fibers could hardly pile into a large disordered phase due to the relatively poorer mobility of the P3HT block. The WAXS and SAXS results were consistent with those from the DSC measurement, indicating the decreased crystallinity and mobility of the P3HT block in P*t*BS$_{89}$/P3HT$_{35}$ Janus fibers in the bulk state.

Finally, the re-self-assembly behavior of P*t*BS$_{89}$/P3HT$_{35}$ Janus fibers (L_n of 242 nm, width of 12 nm, formed from the P*t*BS$_{89}$-*b*-PI$_{68}$-*b*-P3HT$_{35}$ fiber after self-seeding CDSA at 90 °C) was further performed in Hep/Tol (9/1, v/v) cosolvent. Surprisingly, the P*t*BS$_{89}$/P3HT$_{35}$ Janus fibers precipitated, although the original solvent for the self-assembly and stabilization of P*t*BS$_{89}$-*b*-PI$_{68}$-*b*-P3HT$_{35}$ fibers was employed. The reason might be attributed to the inadequate stabilization ability of the P*t*BS block and the poor chain mobility of P3HT in P*t*BS$_{89}$/P3HT$_{35}$ Janus fibers in Hep/Tol (9/1, v/v) cosolvent. Alternatively, the toluene content was increased, and the Hep/Tol (8/2, v/v) cosolvent was employed. As shown in Figure 5a, after annealing at 50 °C, the fibers re-self-assembled by P*t*BS$_{89}$/P3HT$_{35}$ Janus fibers had an L_n of 267 nm and a width of 20 nm. In this case, the width was doubled to that of the P*t*BS$_{89}$/P3HT$_{35}$ Janus fibers while maintaining a similar fiber length. In Figure 5c, the length−frequency distribution had one peak at 200−250 nm. This result indicated that the re-self-assembled fiber was mainly self-assembled by two P*t*BS$_{89}$/P3HT$_{35}$ Janus fibers. After annealing at 90 °C, the re-self-assembled fibers were lengthened to 301 nm and maintained a width of 20 nm (Figure 5b). Differently, in Figure 5d, the length−frequency distribution showed two peaks at 200−250 and 350−400 nm, respectively. The size of the latter peak (350−400 nm) was just double that of the former (200−250 nm), indicating that the re-self-assembled fibers formed at 90 °C statistically existed in the form of 2 or 4 aggregates. Comparatively, the P*t*BS$_{89}$-*b*-PI$_{68}$-*b*-P3HT$_{35}$ fibers annealed at 50 and 90 °C in Hep/Tol (8/2, v/v) cosolvent had longer L_ns of 1070 and 1460 nm, respectively (Figure 5e−h). The intrinsic reason for the shorter length of the re-self-assembled P*t*BS$_{89}$/P3HT$_{35}$ Janus fibers might be attributed to the larger sizes of P*t*BS$_{89}$/P3HT$_{35}$ Janus fibers to the P*t*BS$_{89}$-*b*-PI$_{68}$-*b*-P3HT$_{35}$ triblock copolymer. In the former case, the mobility and crystallinity of P3HT side chains were mostly restricted. Additionally, the UV−vis spectrum for the re-self-assembled P*t*BS$_{89}$/P3HT$_{35}$ Janus fibers in Hep/Tol (8/2, v/v) cosolvent was different from that for P*t*BS$_{89}$/P3HT$_{35}$ Janus fibers in toluene (Figure 5g). In the former case, the peak shifted to a higher wavelength, indicating the enhanced stiffness and aggregation for the P3HT side chains in Hep/

https://doi.org/10.1021/acsmacrolett.5c00525
ACS Macro Lett. 2025, 14, 1367−1374

Tol (8/2, v/v) cosolvent. Meanwhile, the re-self-assembled P*t*BS$_{89}$/P3HT$_{35}$ Janus fibers showed a much weaker absorption at 560 and 605 nm compared to P*t*BS$_{89}$-*b*-PI$_{68}$-*b*-P3HT$_{35}$ fibers in the same Hep/Tol (8/2, v/v) cosolvent, indicating the incomplete crystallization of the P3HT side chain. Thus, unlike the CDSA of P*t*BS$_{89}$-*b*-PI$_{68}$-*b*-P3HT$_{35}$ triblock copolymer, the P*t*BS$_{89}$/P3HT$_{35}$ Janus fibers re-self-assembled by average 2- or 4-aggregates with relatively weak crystallinity. Generally, the higher annealing temperature of 90 °C tended to induce more 4-aggregates, as Figure 5h illustrated.

In summary, we reported a general approach to prepare P3HT-based Janus fibers via the CDSA process. The P*t*BS/P3HT Janus fibers were generated with lengths ranging from 160 to 240 nm, which were close to or slightly shorter than the length of P*t*BS-*b*-PI-*b*-P3HT fibers. As expected, the width of the P*t*BS/P3HT Janus fibers was almost half of that for the P*t*BS-*b*-PI-*b*-P3HT fibers. The P*t*BS/P3HT Janus fibers could further re-self-assemble into 2- or 4-aggregates in selective solvents. Comprehensively, the P*t*BS/P3HT Janus fibers were featured with relatively low chain mobility and crystallinity, potentially facilitating the modulation on properties and functions of P3HT-based copolymers. The approach presented in this work is also expected to facilitate the fabrication of uniform Janus fibers containing π-conjugated polymers and their applications in advanced materials.

■ ASSOCIATED CONTENT

Supporting Information

The Supporting Information is available free of charge at https://pubs.acs.org/doi/10.1021/acsmacrolett.5c00525.

Experimental details and additional characterization data, including Figures S1−S10 (PDF)

■ AUTHOR INFORMATION

Corresponding Author

Guowei Wang − *State Key Laboratory of Molecular Engineering of Polymers, Department of Macromolecular Science, Fudan University, Shanghai 200433, China;* orcid.org/0000-0003-2595-8269; Email: gwwang@fudan.edu.cn

Authors

Boyang Shi − *State Key Laboratory of Molecular Engineering of Polymers, Department of Macromolecular Science, Fudan University, Shanghai 200433, China*

Chengcheng Zhou − *State Key Laboratory of Molecular Engineering of Polymers, Department of Macromolecular Science, Fudan University, Shanghai 200433, China*

Xinyu Wang − *State Key Laboratory of Molecular Engineering of Polymers, Department of Macromolecular Science, Fudan University, Shanghai 200433, China*

Ding Shen − *State Key Laboratory of Molecular Engineering of Polymers, Department of Macromolecular Science, Fudan University, Shanghai 200433, China*

Complete contact information is available at: https://pubs.acs.org/10.1021/acsmacrolett.5c00525

Author Contributions

CRediT: **Boyang Shi** conceptualization, data curation, formal analysis, investigation, methodology, resources, software, validation, visualization, writing - original draft, writing - review & editing; **Chengcheng Zhou** formal analysis, investigation, resources, software, validation, writing - original draft; **Xinyu Wang** data curation, formal analysis, visualization, writing - original draft; **Ding Shen** formal analysis, methodology, software, writing - original draft; **Guowei Wang** conceptualization, funding acquisition, project administration, supervision, writing - review & editing.

Notes

The authors declare no competing financial interest.

■ ACKNOWLEDGMENTS

This work is supported by the National Natural Science Foundation of China (22271058).

■ REFERENCES

(1) Persson, N. E.; Chu, P. H.; McBride, M.; Grover, M.; Reichmanis, E. Nucleation, Growth, and Alignment of Poly(3-hexylthiophene) Nanofibers for High-Performance OFETs. *Acc. Chem. Res.* **2017**, *50* (4), 932−942.

(2) Agbolaghi, S.; Zenoozi, S. A comprehensive review on poly(3-alkylthiophene)-based crystalline structures, protocols and electronic applications. *Org. Electron* **2017**, *51*, 362−403.

(3) Chang, B.; Chen, C. H.; Hsueh, T. F.; Tan, S.; Lin, Y. C.; Zhao, Y. P.; Tsai, B. S.; Chu, T. Y.; Chang, Y. N.; Tsai, C. E.; et al. High-Performance Poly(3-hexyl thiophene)-Based Organic Photovoltaics with Side-Chain Engineering of Core Units of Small Molecule Acceptors. *ACS Appl. Mater. Interfaces* **2023**, *15* (45), 52651−52660.

(4) Huang, S. L.; Ye, C. C.; Pan, Y. N.; Liu, Q. Y.; Wang, C.; Xu, L. Living Direct Arylation Polymerization via C-H Activation for the Precision Synthesis of Polythiophenes and Their Block Copolymers. *Macromolecules* **2025**, *58* (5), 2357−2365.

(5) Tran, Q. D.; Knight, L. R.; Rui, G. C.; Mason, G. T.; Kulatunga, P.; Bushnell, A. J.; Hou, B. W.; Zhu, L.; Rondeau-Gagné, S.; Sauvé, G. Ester Side Chain Functionalization Enhances Mechanical Properties of Poly(3-Hexylthiophene) while Maintaining High Hole Mobility. *Macromolecules* **2024**, *57* (9), 4544−4555.

(6) Chevrier, M.; Lopez, G.; Zajaczkowski, W.; Kesters, J.; Lenaerts, R.; Surin, M.; De Winter, J.; Richeter, S.; Pisula, W.; Mehdi, A.; et al. Synthesis and properties of a P3HT-based ABA triblock copolymer containing a perfluoropolyether central segment. *Synth. Met.* **2019**, *252*, 127−134.

(7) Yu, X.; Xiao, K.; Chen, J. H.; Lavrik, N. V.; Hong, K. L.; Sumpter, B. G.; Geohegan, D. B. High-Performance Field-Effect Transistors Based on Polystyrene-*b*-Poly(3-hexylthiophene) Diblock Copolymers. *ACS Nano* **2011**, *5* (5), 3559−3567.

(8) Fujita, H.; Michinobu, T.; Tokita, M.; Ueda, M.; Higashihara, T. Synthesis and Postfunctionalization of Rod-Coil Diblock and Coil-Rod-Coil Triblock Copolymers Composed of Poly(3-hexylthiophene) and Poly(4-(4'-*N*, *N*-dihexylaminophenylethynyl)styrene) Segments. *Macromolecules* **2012**, *45* (24), 9643−9656.

(9) Peng, R.; Pang, B.; Hu, D. Q.; Chen, M. J.; Zhang, G. B.; Wang, X. H.; Lu, H. B.; Cho, K.; Qiu, L. Z. An ABA triblock copolymer strategy for intrinsically stretchable semiconductors. *J. Mater. Chem. C* **2015**, *3* (15), 3599−3606.

(10) Higashihara, T.; Fukuta, S.; Ochiai, Y.; Sekine, T.; Chino, K.; Koganezawa, T.; Osaka, I. Synthesis and Deformable Hierarchical Nanostructure of Intrinsically Stretchable ABA Triblock Copolymer Composed of Poly(3-hexylthiophene) and Polyisobutylene Segments. *ACS Appl. Polym. Mater.* **2019**, *1* (3), 315−320.

(11) Le Nguyen, T. P.; Bui, T. T.; Nguyen, C. H. T.; Le, D. T.; Nguyen, T. H.; Nguyen, L. T.; Nguyen, Q. T.; Hoang, M. H.; Yokozawa, T.; Nguyen, H. Diblock copolymers poly(3-hexylthiophene)-*random*-poly(2-(dimethylamino)ethyl methacrylate-1-pyrenylmethyl methacrylate), controlled synthesis and optical properties. *J. Polym. Res.* **2023**, *30* (8), 292.

(12) Coulembier, O.; Deshayes, G.; Surin, M.; De Winter, J.; Boon, F.; Delcourt, C.; Leclère, P.; Lazzaroni, R.; Gerbaux, P.; Dubois, P. Macrocyclic regioregular poly(3-hexylthiophene): from controlled

synthesis to nanotubular assemblies. *Polym. Chem.* **2013**, *4* (2), 237−241.
(13) McKeown, G. R.; Fang, Y.; Obhi, N. K.; Manion, J. G.; Perepichka, D. F.; Seferos, D. S. Synthesis of Macrocyclic Poly(3-hexylthiophene) and Poly(3-heptylselenophene) by Alkyne Homocoupling. *ACS Macro Lett.* **2016**, *5* (10), 1075−1079.
(14) Pang, X. C.; Zhao, L.; Feng, C. W.; Lin, Z. Q. Novel Amphiphilic Multiarm, Starlike Coil-Rod Diblock Copolymers via a Combination of Click Chemistry with Living Polymerization. *Macromolecules* **2011**, *44* (18), 7176−7183.
(15) Higashihara, T.; Ito, S.; Fukuta, S.; Miyane, S.; Ochiai, Y.; Ishizone, T.; Ueda, M.; Hirao, A. Synthesis and Characterization of Multicomponent ABC- and ABCD-Type Miktoarm Star-Branched Polymers Containing a Poly(3-hexylthiophene) Segment. *ACS Macro Lett.* **2016**, *5* (5), 631−635.
(16) Okamoto, K.; Housekeeper, J. B.; Michael, F. E.; Luscombe, C. K. Thiophene based hyperbranched polymers with tunable branching using direct arylation methods. *Polym. Chem.* **2013**, *4* (12), 3499−3506.
(17) van As, D.; Subbiah, J.; Jones, D. J.; Wong, W. W. H. Controlled Synthesis of Well-Defined Semiconducting Brush Polymers. *Macromol. Chem. Phys.* **2016**, *217* (3), 403−413.
(18) Ahn, S.-k.; Carrillo, J.-M. Y.; Keum, J. K.; Chen, J.; Uhrig, D.; Lokitz, B. S.; Sumpter, B. G.; Kilbey, S. M. Nanoporous poly(3-hexylthiophene) thin film structures from self-organization of a tunable molecular bottlebrush scaffold. *Nanoscale* **2017**, *9* (21), 7071−7080.
(19) Obhi, N. K.; Jarrett-Wilkins, C. N.; Hicks, G. E. J.; Seferos, D. S. Self-Assembly of Poly(3-hexylthiophene) Bottlebrush Polymers into End-On-End Linear Fiber Morphologies. *Macromolecules* **2020**, *53* (19), 8592−8599.
(20) Lotocki, V.; Battaglia, A. M.; Moon, N.; Titi, H. M.; Seferos, D. S. Conjugated core-shell bottlebrush polymers that exhibit crystallization-driven self-assembly. *Chem. Sci.* **2025**, *16* (2), 920−932.
(21) Sarvari, R.; Agbolaghi, S.; Massoumi, B.; Sorkhishams, N. Electroactive polythiophene/polystyrene bottlebrushes as morphology compatibilizers in photovoltaic systems. *Polym. Int.* **2020**, *69* (4), 397−403.
(22) Ahn, S. K.; Pickel, D. L.; Kochemba, W. M.; Chen, J. H.; Uhrig, D.; Hinestrosa, J. P.; Carrillo, J. M.; Shao, M.; Do, C.; Messman, J. M.; et al. Poly(3-hexylthiophene) Molecular Bottlebrushes via Ring-Opening Metathesis Polymerization: Macromolecular Architecture Enhanced Aggregation. *ACS Macro Lett.* **2013**, *2* (8), 761−765.
(23) Heinrich, C. D.; Thelakkat, M. Poly-(3-hexylthiophene) bottlebrush copolymers with tailored side-chain lengths and high charge carrier mobilities. *J. Mater. Chem. C* **2016**, *4* (23), 5370−5378.
(24) Vatankhah-Varnosfaderani, M.; Keith, A. N.; Cong, Y. D.; Liang, H. Y.; Rosenthal, M.; Sztucki, M.; Clair, C.; Magonov, S.; Ivanov, D. A.; Dobrynin, A. V.; et al. Chameleon-like elastomers with molecularly encoded strain-adaptive stiffening and coloration. *Science* **2018**, *359* (6383), 1509−1513.
(25) Chen, K. R.; Hu, X.; Zhu, N.; Guo, K. Design, Synthesis, and Self-Assembly of Janus Bottlebrush Polymers. *Macromol. Rapid Commun.* **2020**, *41* (20), 2000357.
(26) Xu, B. B.; Feng, C.; Huang, X. Y. A versatile platform for precise synthesis of asymmetric molecular brush in one shot. *Nat. Commun.* **2017**, *8*, 333.
(27) Hils, C.; Schmelz, J.; Drechsler, M.; Schmalz, H. Janus Micelles by Crystallization-Driven Self-Assembly of an Amphiphilic, Double-Crystalline Triblock Copolymer. *J. Am. Chem. Soc.* **2021**, *143* (38), 15582−15586.
(28) Luo, H. Y.; Santos, J. L.; Herrera-Alonso, M. Toroidal structures from brush amphiphiles. *Chem. Commun.* **2014**, *50* (5), 536−538.
(29) Guo, Z. H.; Le, A. N.; Feng, X. D.; Choo, Y.; Liu, B. Q.; Wang, D. Y.; Wan, Z. Y.; Gu, Y. W.; Zhao, J.; Li, V.; et al. Janus Graft Block Copolymers: Design of a Polymer Architecture for Independently Tuned Nanostructures and Polymer Properties. *Angew. Chem., Int. Ed.* **2018**, *57* (28), 8493−8497.
(30) Feng, C.; Huang, X. Y. Polymer Brushes: Efficient Synthesis and Applications. *Acc. Chem. Res.* **2018**, *51* (9), 2314−2323.
(31) Kawamoto, K.; Zhong, M. J.; Gadelrab, K. R.; Cheng, L. C.; Ross, C. A.; Alexander-Katz, A.; Johnson, J. A. Graft-through Synthesis and Assembly of Janus Bottlebrush Polymers from A-*Branch*-B Diblock Macromonomers. *J. Am. Chem. Soc.* **2016**, *138* (36), 11501−11504.
(32) Gröschel, A. H.; Walther, A.; Löbling, T. I.; Schmelz, J.; Hanisch, A.; Schmalz, H.; Müller, A. H. E. Facile, Solution-Based Synthesis of Soft, Nanoscale Janus Particles with Tunable Janus Balance. *J. Am. Chem. Soc.* **2012**, *134* (33), 13850−13860.
(33) Walther, A.; Drechsler, M.; Rosenfeldt, S.; Harnau, L.; Ballauff, M.; Abetz, V.; Müller, A. H. E. Self-Assembly of Janus Cylinders into Hierarchical Superstructures. *J. Am. Chem. Soc.* **2009**, *131* (13), 4720−4728.
(34) Qi, H.; Zhou, T.; Mei, S.; Chen, X.; Li, C. Y. Responsive Shape Change of Sub-5 nm Thin, Janus Polymer Nanoplates. *ACS Macro Lett.* **2016**, *5* (6), 651−655.
(35) Ma, J. Y.; Lu, G. L.; Huang, X. Y.; Feng, C. π-Conjugated-polymer-based nanofibers through living crystallization-driven self-assembly: preparation, properties and applications. *Chem. Commun.* **2021**, *57* (98), 13259−13274.
(36) Yang, H.; Xia, H.; Wang, G. W.; Peng, J.; Qiu, F. Insights into poly(3-hexylthiophene)-b-poly(ethylene oxide) block copolymer: Synthesis and solvent-induced structure formation in thin films. *J. Polym. Sci., Polym. Chem.* **2012**, *50* (24), 5060−5067.
(37) Gwyther, J.; Gilroy, J. B.; Rupar, P. A.; Lunn, D. J.; Kynaston, E.; Patra, S. K.; Whittell, G. R.; Winnik, M. A.; Manners, I. Dimensional Control of Block Copolymer Nanofibers with a -Conjugated Core: Crystallization-Driven Solution Self-Assembly of Amphiphilic Poly(3-hexylthiophene)-*b*-poly(2-vinylpyridine). *Chem.—Eur. J.* **2013**, *19* (28), 9186−9197.
(38) Patra, S. K.; Ahmed, R.; Whittell, G. R.; Lunn, D. J.; Dunphy, E. L.; Winnik, M. A.; Manners, I. Cylindrical Micelles of Controlled Length with a pi-Conjugated Polythiophene Core via Crystallization-Driven Self-Assembly. *J. Am. Chem. Soc.* **2011**, *133* (23), 8842−8845.
(39) Gilroy, J. B.; Lunn, D. J.; Patra, S. K.; Whittell, G. R.; Winnik, M. A.; Manners, I. Fiber-like Micelles via the Crystallization-Driven Solution Self-Assembly of Poly(3-hexylthiophene)-block-Poly(methyl methacrylate) Copolymers. *Macromolecules* **2012**, *45* (14), 5806−5815.
(40) Qian, J. S.; Li, X. Y.; Lunn, D. J.; Gwyther, J.; Hudson, Z. M.; Kynaston, E.; Rupar, P. A.; Winnik, M. A.; Manners, I. Uniform, High Aspect Ratio Fiber-like Micelles and Block Co-micelles with a Crystalline pi-Conjugated Polythiophene Core by Self-Seeding. *J. Am. Chem. Soc.* **2014**, *136* (11), 4121−4124.
(41) Li, X. Y.; Wolanin, P. J.; MacFarlane, L. R.; Harniman, R. L.; Qian, J. S.; Gould, O. E. C.; Dane, T. G.; Rudin, J.; Cryan, M. J.; Schmaltz, T.; Frauenrath, H.; Winnik, M. A.; Faul, C. F. J.; Manners, I. Uniform electroactive fibre-like micelle nanowires for organic electronics. *Nat. Commun.* **2017**, *8*, 15909.
(42) Fukui, T.; Garcia-Hernandez, J. D.; MacFarlane, L. R.; Lei, S. X.; Whittell, G. R.; Manners, I. Seeded Self-Assembly of Charge-Terminated Poly(3-hexylthiophene) Amphiphiles Based on the Energy Landscape. *J. Am. Chem. Soc.* **2020**, *142* (35), 15038−15048.
(43) MacFarlane, L. R.; Li, X. Y.; Faul, C. F. J.; Manners, I. Efficient and Controlled Seeded Growth of Poly(3-hexylthiophene) Block Copolymer Nanofibers through Suppression of Homogeneous Nucleation. *Macromolecules* **2021**, *54* (24), 11269−11280.
(44) Huang, F. F.; Ma, J. Y.; Nie, J. C.; Xu, B. B.; Huang, X. Y.; Lu, G. L.; Winnik, M. A.; Feng, C. A Versatile Strategy toward Donor-Acceptor Nanofibers with Tunable Length/Composition and Enhanced Photocatalytic Activity. *J. Am. Chem. Soc.* **2024**, *146* (36), 25137−25150.
(45) Yokoyama, A.; Miyakoshi, R.; Yokozawa, T. Chain-growth polymerization for poly(3-hexylthiophene) with a defined molecular weight and a low polydispersity. *Macromolecules* **2004**, *37* (4), 1169−1171.

https://doi.org/10.1021/acsmacrolett.5c00525
ACS Macro Lett. 2025, 14, 1367−1374

(46) Lim, H.; Chao, C. Y.; Su, W. F. Modulating Crystallinity of Poly(3-hexylthiophene) via Microphase Separation of Poly(3-hexylthiophene)-Polyisoprene Block Copolymers. *Macromolecules* **2015**, *48* (10), 3269−3281.
(47) Tao, D. L.; Feng, C.; Cui, Y. A.; Yang, X.; Manners, I.; Winnik, M. A.; Huang, X. Y. Monodisperse Fiber-like Micelles of Controlled Length and Composition with an Oligo(*p*-phenylenevinylene) Core via ″Living″ Crystallization-Driven Self-Assembly. *J. Am. Chem. Soc.* **2017**, *139* (21), 7136−7139.
(48) Tao, D. L.; Wang, Z. Q.; Huang, X. Y.; Tian, M. W.; Lu, G. L.; Manners, I.; Winnik, M. A.; Feng, C. Continuous and Segmented Semiconducting Fiber-like Nanostructures with Spatially Selective Functionalization by Living Crystallization-Driven Self-Assembly. *Angew. Chem., Int. Ed.* **2020**, *59* (21), 8232−8239.
(49) Hayward, D. W.; Lunn, D. J.; Seddon, A.; Finnegan, J. R.; Gould, O. E. C.; Magdysyuk, O.; Manners, I.; Whittell, G. R.; Richardson, R. M. Structure of the Crystalline Core of Fiber-like Polythiophene Block Copolymer Micelles. *Macromolecules* **2018**, *51* (8), 3097−3106.
(50) Liu, J. H.; Arif, M.; Zou, J. H.; Khondaker, S. I.; Zhai, L. Controlling Poly(3-hexylthiophene) Crystal Dimension: Nanowhiskers and Nanoribbons. *Macromolecules* **2009**, *42* (24), 9390−9393.
(51) Pietrasik, J.; Sumerlin, B. S.; Lee, H. I.; Gil, R. R.; Matyjaszewski, K. Structural mobility of molecular bottle-brushes investigated by NMR relaxation dynamics. *Polymer* **2007**, *48* (2), 496−501.
(52) Scoti, M.; De Stefano, F.; Zanchin, G.; Leone, G.; De Rosa, C.; Ricci, G. Synthesis, Structure, and Properties of Poly(isoprene)s of Different Constitutions and Configurations from Catalysts Based on Complexes of Nd, Co, and Fe. *Macromolecules* **2023**, *56* (12), 4629−4638.

https://doi.org/10.1021/acsmacrolett.5c00525
ACS Macro Lett. 2025, 14, 1367−1374